American Mineralogist, Volume 86, pages 1219–1230, 2001

The crystal chemistry of birefringent natural uvarovites: Part I. Optical investigations and UV-VIS-IR absorption spectroscopy

MICHAEL ANDRUT AND MANFRED WILDNER*

Institut für Mineralogie und Kristallographie, Universität Wien, Geozentrum, Althanstrasse 14, A-1090 Wien, Austria

ABSTRACT

Six garnet crystals with compositions close to the uvarovite-grossular binary from three different localities (Saranov, Veselovsk, and Saranka, Ural Mountains, Russia) were investigated by optical methods, electron microprobe analysis, and polarized UV-VIS-IR micro-spectroscopy. Under crossed polarizers the crystals display "strong" birefringence in the order of 0.006 and formation of domains, aligned parallel to the crystal faces of the form {110}. Referring to the cubic cell, *Y* is always parallel to a principal lattice direction, e.g., $[010]_{cub}$, whereas *X* and *Z* are then parallel to $[101]_{cub}$ and $[10\bar{1}]_{cub}$, respectively.

The garnets are uvarovite-grossular solid solutions with 48 to 71 mol% uvarovite component and traces of Ti, Fe, Mn, and Mg, and exhibit no compositional zoning.

Polarized single crystal infrared absorption spectra in the region of the OH stretching vibration display 14 discernible, partly superimposing, and strongly anisotropic absorption bands between 3470 and 3680 cm^{-1}, which are caused by structurally incorporated hydroxyl groups. The polarization behavior observed for individual samples complies with orthorhombic, monoclinic, and triclinic crystal symmetry, respectively. The water content calculated using an integral extinction coefficient, $\varepsilon = 43800$ L/cm^2·mol, ranges from 0.07 to 0.34 wt%. Annealing experiments indicate that the incorporation of hydroxyl groups is not the primary cause for the anisotropic behavior. Instead, cation ordering on octahedral positions may play an important role. This assumption is substantiated by single crystal X-ray diffraction investigations reported in Part II of the present study (Wildner and Andrut 2001).

Contrary to the IR spectroscopic data, single-crystal electronic absorption spectra show no significant polarization behavior in the UV-VIS-NIR spectral region. The observed absorption bands are caused by *d-d* transitions of Cr^{3+} cations in octahedral coordination. The linear extinction coefficients of the investigated uvarovites strongly indicate that the Cr^{3+} cations occupy centrosymmetric sites, regardless of the exact symmetry reduction from $Ia\bar{3}d$.

INTRODUCTION

Natural garnets in general, but especially those belonging to the grossular-andradite series, often exhibit weak birefringence. Various reasons for this anomalous optical behavior of normally cubic garnets are discussed in the literature (e.g., Akizuki 1984; Allen and Buseck 1988; Kingma and Downs 1989; Hofmeister et al. 1998). These include:

(1) Plastic deformation (Allen and Buseck 1988).

(2) Substitution of rare-earth cations for Ca, resulting in magneto-optical effects (Blanc and Maissoneuve 1973).

(3) Residual strain from lattice mismatch at compositional, twin or grain boundaries (Chase and Lefever 1960; Lessing and Standish 1973; Kitamura and Komatsu 1978; Foord and Mills 1978; Akizuki 1984; Hofmeister et al. 1998). In their investigation of 48 optically anisotropic garnets, Hofmeister et al. (1998) found that strain is accompanied by low birefringence with δ up to 0.0006 and undulatory extinction.

(4) Large scale twinning (Ingerson and Barksdale 1943; Brown and Mason 1994).

(5) Reduction of symmetry due to ordering of cations on octahedral (Al and Fe^{3+}: Takéuchi et al. 1982; Akizuki 1984; Allen and Buseck 1988; Akizuki et al. 1998) and/or on dodecahedral sites (Ca and Fe^{2+}: Kingma and Downs 1989; Griffen et al. 1992).

(6) Presence of OH groups which are distributed in a non-cubic manner (Rossman and Aines 1986).

Most natural garnets with anisotropic properties studied so far belong to the grossular-andradite series (Takéuchi et al. 1982; Akizuki 1984; Aines and Rossman 1984; Allen and Buseck 1988; McAloon and Hofmeister 1993; Akizuki et al. 1998). In contrast, natural garnets with a significant uvarovite component have only occasionally been subject to detailed investigations. The structure of an isotropic near end-member uvarovite from Washington (California) was refined by Novak and Gibbs (1971). Von Knorring (1951) reported both optically isotropic and anisotropic uvarovites from Outokumpu (Finland). Foord and Mills (1978) attempted to explain the anomalous optical properties of several mineral species, but for their uvarovite sample no explanation was given.

Chromium-rich garnets were the subject of a number of UV-VIS spectroscopic absorption studies, but unfortunately few authors also gave complete chemical analyses, so that the spectral data could be quantitatively interpreted and compared

* E-mail: manfred.wildner@univie.ac.at

0003-004X/01/0010–1219$05.00

(Neuhaus 1960; Manning 1969; Moore and White 1972; Langer and Abu-Eid 1977; Taran et al. 1994). Diffuse reflectance spectra of uvarovites from Outokumpu were reported by Amthauer (1976). He described the corresponding spin-allowed Cr^{3+} *d-d* transitions as asymmetric. Nevertheless, all these Cr-bearing garnets were reported to be cubic.

In contrast, IR spectroscopic investigations of the OH stretching vibrational region of uvarovites are scarce (Heflik and Zabinski 1969), despite the fact that the hydrous component of garnets is of interest for several reasons.

(1) Even a minor water component in nominally anhydrous phases has an important influence on their physical and chemical properties, e.g., on the rheological behavior of rocks, and on deformation mechanisms, and has to be considered in thermodynamic calculations applied to geothermobarometry (Griggs and Blacic 1964).

(2) Traces of hydroxyl in garnets can serve, due to their abundance, as an important water reservoir in the upper mantle (Martin and Donnay 1972; Thompson 1992).

(3) The water content of these minerals controls the water fugacity of a coexisting fluid phase (Aines and Rossman 1984, 1985).

(4) Hydroxyl zoning in metamorphic hydrogrossular may give information about *P-T* paths during growth (Lager et al. 1989).

A hydrous component has been established in both synthetic and natural garnets of various compositions (Aines and Rossman 1984; Geiger et al. 1989, 1991; Rossman and Aines 1991). The mechanism of incorporation via the hydrogarnet substitution $(OH)_4^{4-} \leftrightarrow SiO_4^{4-}$ has been well characterized by X-ray and neutron diffraction and by IR spectroscopy (Cohen-Addad et al. 1964, 1967; Foreman 1968; Kobayashi and Shoji 1983; Lager et al. 1987, 1989). However, other mechanisms for the incorporation of OH are also debated (Basso et al. 1984; Langer et al. 1993; Khomenko et al. 1994; Geiger et al. 2000).

The present paper reports polarized single crystal IR- and UV-VIS absorption spectra obtained on optically clear sections of six birefringent garnet samples from three different localities (Saranov, Veselovsk and Saranka, Ural Mountains, Russia). We selected natural garnet samples representing, to a first approximation, a simple binary of the grossular-uvarovite join with predominant uvarovite component. Such a simple composition was chosen to avoid a significant influence of additional cations to the IR spectra. Our aim is to propose a noncubic structure of the investigated garnets, and to identify the factors causing their anisotropic behavior. Furthermore, due to their actual structural deviation from cubic symmetry (cf., Andrut and Wildner 2001), these uvarovites are the basis for both the explanation of the incorporation mechanisms of hydroxyl groups and their orientation in the garnet structure. An important goal of this study was to prove that the incorporated hydroxyl groups obey certain symmetries, a fact that has not previously been studied in detail (Rossman and Aines 1986; Allen and Buseck 1988). In Part II (Wildner and Andrut 2001), these results are compared with those obtained in single crystal X-ray structure investigations.

Sample description

Chromium-dominant grossular-uvarovite solid solutions from the Russian localities of Saranov, Saranka and Veselovsk (Ural Mountains) were studied. At all localities, idiomorphic single crystals grow in fissures and fractures of a chromite ore body associated with gabbros and peridotites (Pavlov and Grigore'eva 1977). The crystals are up to 4 mm in diameter, dark green in color and exhibit a dodecahedral form. There is no evidence that the host rock has been deformed, so the crystals were probably not strained externally after growth. Therefore, all optical properties and internal textures are expected to be of primary origin.

Experimental details

Thin sections (~75 μm thick) were prepared parallel to a face of the cubic {110} form. Optical investigation under crossed polarizers revealed clear birefringence and the formation of domains up to 1 mm in size and aligned parallel to the crystal faces of the {110} form. One optical extinction position is always parallel to a principal cubic lattice direction, e.g., [010], whereas the remaining two extinctions are then aligned parallel to [101] and $[10\bar{1}]$, respectively.

In some sections, the central domain exhibits a "bowtie" structure with four sectors, a feature that was also mentioned by Akizuki (1984) and Allen and Buseck (1988) in grossular-andradite solid solutions. Only optically homogeneous, inclusion-free fragments of the crystals with clear extinction positions under crossed polarizers were examined, i.e., samples with "bowtie" structures or laminated textures were excluded. Approximate cubes with edge lengths of about 75 μm, free of any inclusions or indications of strain were cut from each of one single domain. The faces of the cubes were polished for the subsequent optical and spectroscopic measurements. From the Saranov locality, cubes were cut from four different crystals (Sar-desy, Sar-kl2, Sar-899, Sar-w2), and from Saranka and Veselovsk one cube each was prepared (Ska-1 and Ves-2, respectively). Samples Sar-kl2, Sar-899, and Sar-w2 were prepared such that each indicatrix axis is perpendicular to a cube face. The optical indicatrix was investigated using a spindle stage. Since the samples show no variable or undulatory extinction, quantitative measurements of retardation (Δ) could be performed with a Berek compensator. The size, orientation and birefringence of the samples are compiled in Table 1.

Electron microprobe analysis

Electron microprobe (EMP) analyses were done on polished and carbon coated samples at the Museum of Natural History, Vienna, with a JEOL ARL-SEMQ microprobe using the following standards: natural garnet (Si, Al, Fe, Mg), kaersutite (Ti), chromite (Cr), jadeite (Na), tephroite (Mn), and augite (Ca). The electron beam diameter was 2 μm with acceleration voltage of 15 kV and beam current of 15 nA. To check the homogeneity of the samples, profiles were measured across thin sections as well as selected spots on the individual prepared cubes.

TEM investigations

Selected-area electron-diffraction (SAED) experiments, bright field images and high-resolution lattice fringe images were done on ion-milled foils with a Philips CM200 transmission electron microscope at the GFZ Potsdam.

TABLE 1. The size, orientation, and birefringence of the prepared uvarovite sample cubes

	Sample					
	Sar-w2	Sar-899	Sar-kl2	Sar-desy	Ska-1	Ves-2
Size (μm)	60×60×68 _	56×60×168 _	80×84×120 _	78×80×86	96×96×144	74×82×94
Orientation	(010), (101), (101)	(010), (101), (101)	(010), (101), (101)	random	random	random
Birefringence						
n_γ-n_α	0.00623(13)	0.00378(13)	0.00657(13)	n.d.*	n.d.	n.d.
n_γ-n_β	0.00236(10)	0.00157(10)	0.00250(10)	n.d.	n.d.	n.d.
n_β-n_α	0.00387(10)	0.00221(10)	0.00407(11)	n.d.	n.d.	n.d.

* n.d. = not determined

Absorption spectroscopic investigations

Polarized absorption spectra were measured at room temperature in the UV-VIS range between 28000 cm^{-1} and 10000 cm^{-1} and in the OH stretching vibrational range between 4000 cm^{-1} and 3000 cm^{-1} using a Bruker IFS 66v/S FTIR-Spectrometer with an attached mirror optics IR microscope. The spectral bandwidth was 20 cm^{-1} in the visible range and 1 cm^{-1} in the infrared range, and the local resolution was 60 μm in both spectral regions. Appropriate combinations of light sources (globar, tungsten lamp, Xe-lamp), beam splitters (KBr, quartz), detectors (MCT, Si-diode, Ge-diode, GaP-diode), and polarizers (KRS-5, calcite Glan-prism) were used. For the weak signal of sample Sar-899, the polarized IR spectra were recorded in the sample chamber using a micro focusing unit. The sample chamber was evacuated to 200 Pa, and consequently the absorption caused by ambient H_2O and CO_2 is of minor influence in the infrared spectral region. Spectra were averaged over 2048 scans in the UV-VIS range and 128 scans in the IR range. Phase correction mode of the interferogram was performed with a procedure after Mertz (cf., Griffiths and de Haseth 1986). Norton-Beer weak mode was chosen as an apodization function. The spectra recorded with different instrumental configurations were fitted together, corrected for the sample thickness, and displayed with linear absorption coefficient α as a function of wave number ν. After background correction, the spectra were resolved into Gaussian- and Lorentzian-shaped absorption bands and their band center, full width at half maximum (FWHM) and integral intensity were determined with the program *PeakFit* by Jandel Scientific.

Three samples from the Saranov locality were selected due to their different water content (Sar-kl2 > Sar-w2 > Sar-899) for detailed study of the polarization behavior of the hydroxyl vibrational bands. In these crystals, the axes of the indicatrix are aligned perpendicular to the faces of the prepared cubes and hence each face contains two indicatrix axes, either (*X, Y*), (*X, Z*), or (*Y, Z*). Spectra for each of two faces were then measured by rotating the samples against the polarizer over a range of 180° in steps of 10°. After band deconvolution, the respective integral intensities were plotted vs. the degree of rotation with respect to the main indicatrix axes. The resulting lemniscate curves are discussed below. Additional measurements at 93 K were performed to check for possible splitting of the OH stretching vibrational bands. Subsequently, sample Sar-w2 and some other crystal platelets were heated up to 1000 °C in air for up to 350 h (Sar-w2t). Then the IR absorption measurements were repeated at ambient conditions.

RESULTS

Electron microprobe analysis

The average values of four analyses per prepared crystal are summarized in Table 2. The EMP analyses reveal that the garnets from all the localities are chemically homogenous. Therefore, compositional zoning can be ruled out as a possible reason for optical anisotropy. The EMP data confirmed that these garnets are, to a good approximation, simple binary uvarovite-grossular solid solutions.

The numbers of cations were calculated on the basis of 12 O atoms; Fe and Ti were considered as $^{[6]}Fe^{3+}$ and $^{[6]}Ti^{4+}$, respectively, which is also supported by the results of the X-ray structure investigations (Part II), and Mn was calculated as Mn^{2+}. The sample from Saranka exhibits the lowest Cr content with 48 mol% uvarovite component, followed by the sample from Veselovsk (66 mol%). The samples from Saranov have the highest Cr contents, showing compositional variation between 68 and 71 mol% uvarovite.

TABLE 2. Mean values of the chemical composition from EMP analyses (wt%) and resulting site occupancies for the investigated uvarovite samples

Wt%	Sample					
oxides	Sar-w2	Sar-899	Sar-kl2	Sar-desy	Ska-1	Ves-2
SiO_2	37.26	36.85	36.35	36.69	37.44	37.02
TiO_2	0.62	0.59	1.11	1.28	0.24	0.95
Cr_2O_3	21.27	21.56	21.41	21.90	15.23	20.40
Al_2O_3	6.35	6.04	5.75	5.33	10.17	6.49
Fe_2O_3	0.13	0.13	0.13	0.08	1.11	0.10
MnO	0.01	0.04	0.01	0.06	0.22	0.02
MgO	0.01	0.03	0.01	0.03	0	0.04
CaO	34.13	34.08	33.89	33.99	34.35	33.89
Total	99.79	99.32	98.66	99.34	98.76	98.90
			site occupancy			
$^{[4]}Si$	3.01	3.00	2.98	2.99	3.01	3.01
Ti^{4+}	0.04	0.04	0.07	0.08	0.01	0.06
Cr^{3+}	1.36	1.39	1.39	1.41	0.97	1.31
Al	0.60	0.58	0.56	0.51	0.96	0.62
Fe^{3+}	0.01	0.01	0.01	<0.01	0.07	0.01
$^{[6]}\Sigma$	2.01	2.02	2.03	2.00	2.01	2.00
Mn^{2+}	<0.01	<0.01	<0.01	<0.01	0.02	<0.01
Mg	<0.01	<0.01	<0.01	<0.01	<0.01	<0.01
Ca	2.95	2.97	2.98	2.98	2.95	2.95
$^{[8]}\Sigma$	2.95	2.97	2.98	2.98	2.97	2.95
Total *	7.97	7.99	7.99	7.97	7.99	7.96

* The number of cations is calculated on the basis of 12 O atoms.

Optical and TEM investigations

Spindle stage measurements of single domains revealed that the garnets are optically biaxial. Referring to the cubic cell, *Y* is always parallel to a principal lattice direction, e.g., [010], whereas *X* and *Z* are oriented parallel to [101] and [10$\bar{1}$], respectively. Optical data for samples Sar-kl2, Sar-899, and Sar-w2 are summarized in Table 1. The birefringence (δ) is in the order of 0.006 for Sar-kl2 and Sar-w2. Sar-899 shows a smaller birefringence of 0.004.

The SAED patterns gave no evidence of a deviation from cubic symmetry. HRTEM images exhibit no indications for the occurrence of micro-twinning.

UV-VIS absorption spectra

In the investigated crystals, Cr is the only transition element in sufficient concentration to give rise to absorption bands due to electronic *d-d* transitions. Possible spectral features caused by Ti, Fe, and Mn are below the detection limit.

In the garnet structure with space group $Ia\bar{3}d$, Cr^{3+} occupies the octahedrally coordinated 16*a* site with point symmetry $\bar{3}$. However, as indicated by the optical investigations and confirmed by the single-crystal X-ray structure refinements (Wildner and Andrut 2001), the site symmetry of the Cr^{3+} cations is reduced in the investigated uvarovite samples. With respect to the possible subgroups and their settings, the new site symmetry is $\bar{1}$ in any case. Depending upon the remaining symmetry, the former unique octahedral site is split into two (orthorhombic), four (monoclinic), or eight (triclinic symmetry) sites (Wildner and Andrut 2001).

As a representative example, the polarized UV-VIS spectra for sample Sar-w2 recorded parallel to the three indicatrix axes are displayed in Figure 1. They are characterized by two intense absorption bands at 16250 and 22600 cm^{-1}, which are typical for Cr^{3+} octahedrally coordinated by O atoms (Tanabe and Sugano 1954; Lever 1984). The spectra do not show any significant pleochroism. The bands show a slight asymmetric shape, but no energy splittings are observed. Therefore, the spectra were interpreted on the basis of an effective local crystal field with O_h ($m\bar{3}m$) symmetry.

The energies of various d^n terms and the respective transitions may be described in terms of the Racah parameters *B* and *C* (Racah 1942) and the crystal field splitting parameter 10 *Dq*. For a detailed description of the algebraic transformation of these equations and of crystal field parameters the reader is referred to the literature (Ballhausen 1962; Lever 1984; Burns 1993). For a d^3 electron configuration and octahedral coordination, the first spin-allowed transition $^4A_{2g}(^4F) \rightarrow {}^4T_{2g}(^4F)$ is equivalent to the crystal field splitting parameter 10 *Dq*. B_{35} is a measure of the degree of interelectronic *d-d* repulsion and is derived from the following relationship:

$$B_{35} = (2\,\nu_1 - \nu_2)(\,\nu_2 - \nu_1)/(27\,\nu_1 - 15\,\nu_2) \quad (1)$$

with ν_1 representing the first and ν_2 the second spin-allowed *d-d* transition. The crystal field stabilization energy for Cr^{3+} in an crystal field with O_h symmetry is calculated from:

$$CFSE_{Cr^{3+}} = 6/5\ 10\ Dq \quad (2)$$

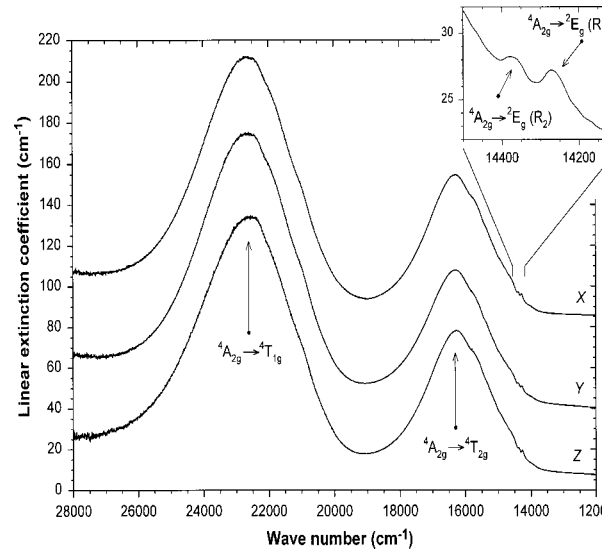

FIGURE 1. Polarized UV-VIS absorption spectra of sample Sar-w2 and assignment of *d-d* transitions of Cr^{3+}. The absorptions show an isotropic behavior. Spectra are offset for clarity. The insert enlarges the spectral range 14100 to 14500 cm^{-1}, displaying the spin-forbidden $^4A_{2g} \rightarrow {}^2E_g(^2G)$ transition split by spin-orbit coupling.

The absorption bands located around 16220 and 22690 cm^{-1} with typical full widths at half maximum of 2200 cm^{-1} and 3200 cm^{-1} are assigned to the spin-allowed *d-d* transitions $^4A_{2g}(^4F) \rightarrow {}^4T_{2g}(^4F)$ and $^4A_{2g}(^4F) \rightarrow {}^4T_{1g}(^4F)$, respectively. At their low energy tails, they exhibit shoulders at 14560, 15340, 15750, 21050, and 22000 cm^{-1}. The third spin-allowed transition $^4A_{2g}(^4F) \rightarrow {}^4T_{1g}(^4P)$ is hidden under the absorption edge which represents the low energy tail of an intense absorption caused by metal-oxygen charge transfer. Based on crystal field calculations with the program TETRIG (Wildner 1996), employing the energy matrices given by Perumareddi (1967), the energy of this third spin-allowed transition $^4A_{2g} \rightarrow {}^4T_{1g}(^4P)$ is calculated to be 35700 cm^{-1}.

Furthermore, a spin-forbidden quartet → doublet transition is clearly observed in the optical spectra. Sharp peaks at 14260 and 14370 cm^{-1} are attributed to components of the $^2E_g(^2G)$ level, split due to spin-orbit coupling. The data for the investigated garnets are summarized in Table 3.

In addition to ligands, type, and symmetry of the coordination polyhedron, the crystal field splitting parameter 10 *Dq* is determined by the mean $3d^n$ ion to ligand distance. In the case of octahedral fields of oxygen ligands with effective charge Z_L, crystal field theory yields:

$$10\ Dq = 5/3\ Z_L\ e^2 \langle r^4 \rangle\ R^{-5} \quad (3)$$

(Lever 1968), where $\langle r^4 \rangle$ is the mean fourth power of the radial distance of an orbital from the nucleus of the central ion, *e* is the charge of an electron and *R* is the mean cation–ligand distance.

This equation is appropriate to compare mean distances

TABLE 3. Energies (cm^{-1}) of the bands caused by $^{[6]}Cr^{3+}$ *d-d* transitions*, calculated crystal field stabilization energies CFSE, crystal field parameters 10*Dq*, and Racah parameters B_{35} (cm^{-1}) for the investigated uvarovite samples

Sample	$^4A_{2g} \rightarrow {}^4T_{2g}(^4F)$	$^4A_{2g} \rightarrow {}^4T_{1g}(^4F)$	$^4A_{2g} \rightarrow {}^4T_{1g}(^4P)$†	$^4A_{2g} \rightarrow {}^2E_g(^2G)$ R_1	$^4A_{2g} \rightarrow {}^2E_g(^2G)$ R_2	*Dq*	Racah B_{35}	$CFSE^{[6]Cr3+}$
Sar-w2	16235	22710	35700	14262	14368	1624	647	19488
Sar-899	16240	22630	35620	14262	14366	1624	636	19488
Sar-kl2	16220	22640	35615	14264	14365	1622	640	19460
Sar-desy	16200	22630	35590	14262	14368	1620	641	19441
Ves-2	16235	22640	35630	14260	14367	1624	638	19488
Ska-1	16310	22650	35700	14264	14368	1631	628	19573

* Notation according to a crystal field with O_h symmetry.
† Calculated.

between central $3d^n$ ions and their ligands from spectroscopically determined values of 10 *Dq*. Considering one type of transition metal ion in one and the same structural type, the product $5/3\ Z_L\ e^2\ <r^4>$ is constant in a solid solution series to a first approximation (Schläfer and Gliemann 1980). An increase of the bulk chromium content generally expands the octahedral sites in the structure (Wildner and Andrut 2001) by replacing Al with larger Cr^{3+} cations. At the same time, the crystal field strength is reduced due to the larger mean interatomic distances, thus shifting the first spin-allowed *d-d* absorption band $^4A_{2g} \rightarrow {}^4T_{2g}$ to lower wave numbers. The Cr content in the samples investigated ranges from 48 to 71 mol% uvarovite component, and this variation results in a band shift of 130 cm^{-1} for the first spin-allowed transition. Similarly, the second spin-allowed transition is also shifted to lower wave numbers with increasing Cr^{3+} content, but with a different slope due to configurational interaction with the $^4T_{1g}(^4P)$ state of alike symmetry. Contrarily, the spin-forbidden transitions are crystal field independent to a first approximation (Table 3), which is also in accordance with the corresponding Tanabe-Sugano diagrams (Tanabe and Sugano 1954).

IR spectra

The polarized IR absorption spectra of samples Sar-kl2, Sar-899, and Sar-w2 were measured parallel to the indicatrix axes and are displayed in Figure 2a–c. The spectra for Sar-desy, Ves-2, and Ska-1 (Fig. 2d) were also recorded with polarized light, but not parallel to their indicatrix axes, due to the different orientation of the prepared cubes. Hence, these latter spectra consist of contributions from at least two indicatrix axes and consequently do not yield correct linear extinction coefficients. In these cases, only one spectrum per sample is shown. In the region of the OH stretching vibrational mode, all spectra are characterized by a system of 14 discernible bands showing a distinct polarization behavior and a flat and constant baseline. Since the spectra were recorded on homogenous and inclusion-free samples, the absorption patterns are evidently intrinsic to these uvarovite garnets. The energies of the bands range from 3680 to 3470 cm^{-1}, which is typical for structurally incorporated hydroxyl groups with weak hydrogen bonds (Libowitzky 1999). The barycenter of the band system is located at 3575 cm^{-1}. Despite their different polarization behavior, as a significant feature all spectra exhibit five groups of bands, which are

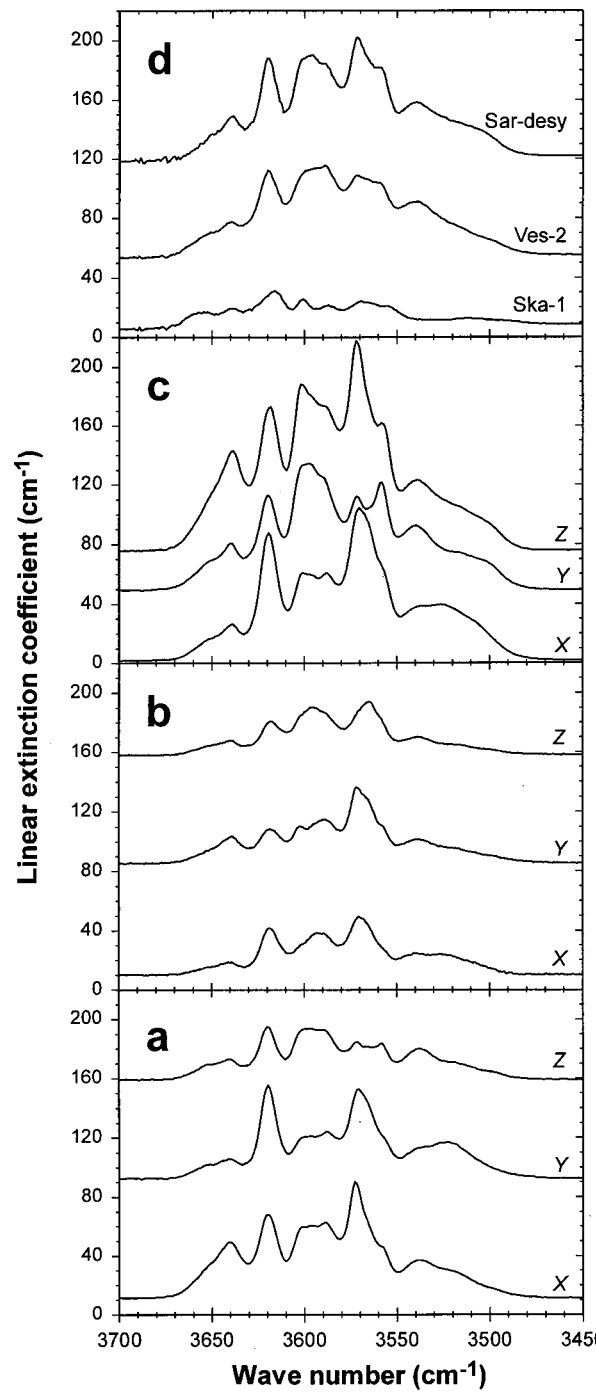

FIGURE 2. Polarized IR absorption spectra of uvarovite **(a)** Sar-w2, **(b)** Sar-899, **(c)** Sar-kl2, recorded parallel to the indicatrix axes and **(d)** polarized spectra with random orientation for Sar-desy, Ves-2 and Ska-1. Spectra are offset for clarity.

separated from each other by absorption minima around 3550, 3580, 3610, and 3630 cm^{-1}. Reasonable starting values for the peak deconvolution process were extracted from bands with highest intensity and weak superposition by neighboring absorptions. The resulting band widths and positions are consistent for all six uvarovite samples. Therefore, in the final stages of the peak fit procedure, band energies and FWHM were constrained to identical values for all samples and only the amplitudes of the bands were varied. The following positions of the peak centers were determined in the deconvolution process: 3502, 3516, 3529, 3541, 3558, 3565, 3572, 3581, 3588, 3596, 3602, 3620, 3640, and 3654 cm^{-1}. FWHM for Gaussian bands was constrained to 15 cm^{-1} and for Lorentzian bands to 10 cm^{-1}. The resulting integral intensities were subsequently used to study the polarization behavior of Sar-kl2, Sar-899, and Sar-w2.

Measurements performed at 93 K did not significantly decrease the band widths and gave no indication of further band splitting. Only a slight band shift of at most ±5 cm^{-1} was observed.

The polarized absorption spectra of sample Sar-w2 before and after annealing at 1000 °C in air for 350 hours (Sar-w2t) are shown in Figure 3. After heat treatment all but four bands had disappeared. The remnant bands are located at 3517, 3556, 3574, and 3602 cm^{-1} and exhibit isotropic behavior. The integral band intensity decreased to approximately 6% of the initial value. Nevertheless, this garnet still behaves optically anisotropically and shows no significant change in birefringence.

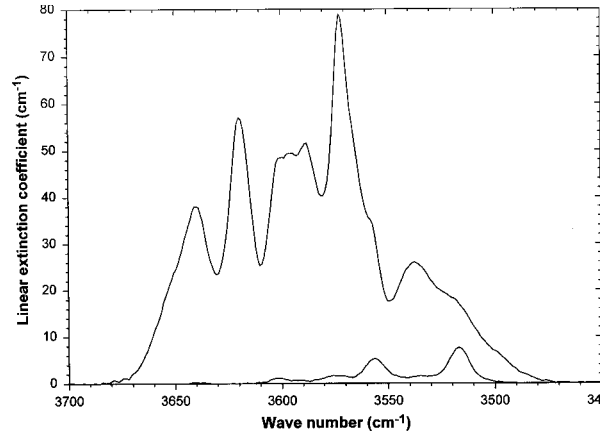

FIGURE 3. Polarized IR spectrum of sample Sar-w2 parallel to the indicatrix axis *X* before and after annealing for 350 hours at 1000 °C. After heating the absorption behavior in the OH vibrational range is isotropic.

IR-polarization behavior

The polarization behavior of samples Sar-kl2, Sar-899, and Sar-w2 is depicted in Figure 4 in the form of the corresponding lemniscate curves of five representative bands. With respect to the indicatrix axes, isotropic, straight, or oblique polarization behavior is discernible for each single absorption band. The analysis of the three-dimensional polarization behavior of the whole band system restricts the possible symmetries of the optically biaxial uvarovites to orthorhombic, monoclinic, or triclinic symmetry.

Sample Sar-899 (Figs. 4c and 4d) shows only isotropic or straight orientation of the lemniscates in both planes, thus obeying orthorhombic symmetry. Sar-kl2 (Figs. 4e and 4f) exhibits isotropic, straight and—for the strongest absorption bands—also oblique orientation in the *XY* plane. This is in accordance with monoclinic symmetry, where the indicatrix axis *Z* is aligned parallel to the monoclinic **b**-axis, i.e., parallel to the cubic [10$\bar{1}$] direction (this orientation corresponds to the monoclinic "mon III" cell setting as defined in Part II). Sar-w2 (Figs. 4a and 4b) is an example where the orientation of the OH dipoles can only be described by triclinic symmetry, since several lemniscates are aligned obliquely with respect to the indicatrix axes in both planes. Hence, judging from the polarized IR absorption measurements in the OH stretching vibrational region, we assign orthorhombic, monoclinic, and triclinic as highest possible symmetries to the Sar-899, Sar-kl2, and Sar-w2 crystals, respectively.

Water component

The total integral absorption intensity α_i, i.e., the sum of absorbances in all three orthogonal polarizations of a crystal (Libowitzky and Rossman 1997), is compiled for the investigated uvarovite crystals in Table 4. The water content is calculated using the following relationship (Beran et al. 1993):

$$c_{H_2O}\ (wt\%) = (1.8\ \alpha_i)/(\varepsilon_i\ D) \quad (4)$$

where ε_i (L/cm^2·mol) is the total integral extinction coefficient and D (g/cm^3) is the density. ε_i is a material constant and has to be calibrated by an independent method. Libowitzky and Rossman (1997) used IR absorption data from polarized measurements of various minerals with stoichiometric water contents to establish a linear calibration curve for water in minerals. This calibration curve agrees with quantitative IR data for staurolite (Koch-Müller et al. 1995) and trace OH-contents in pyroxenes (Bell et al. 1995), but deviates appreciably from those of OH-bearing pyrope (Bell et al. 1995). Lately, quantitative data for grossular-dominant garnets based on nuclear reaction analyses were presented by Hösch (1999). Since these analyses seem to be the most reliable of the ugrandite series, we compared them with the calibration curve by Libowitzky and Rossman (1997). Figure 5 shows that these data are consistent with the calibration curve, indicating its applicability to Ca-bearing garnets with low Fe concentrations.

TABLE 4. Integral intensities of the band system in the OH-vibrational range and calculated water contents* for the investigated uvarovite samples

Sample	α_i (cm^{-2})	*D* (g/cm^3)†	H_2O (wt%)*
Sar-w2	12326	3.774	0.17
Sar-899	7706	3.778	0.11
Sar-kl2	24427	3.777	0.34
Sar-desy	23975	3.783	0.33
Ves-2	22141	3.766	0.31
Ska-1	5046	3.736	0.07

* Calculated using an integral absorption coefficient of ε = 43800 L/cm^2·mol for the barycenter of the band system ν = 3575 cm^{-1} (Libowitzky and Rossman 1997).
† Densities from single crystal X-ray investigations (Wildner and Andrut 2001).

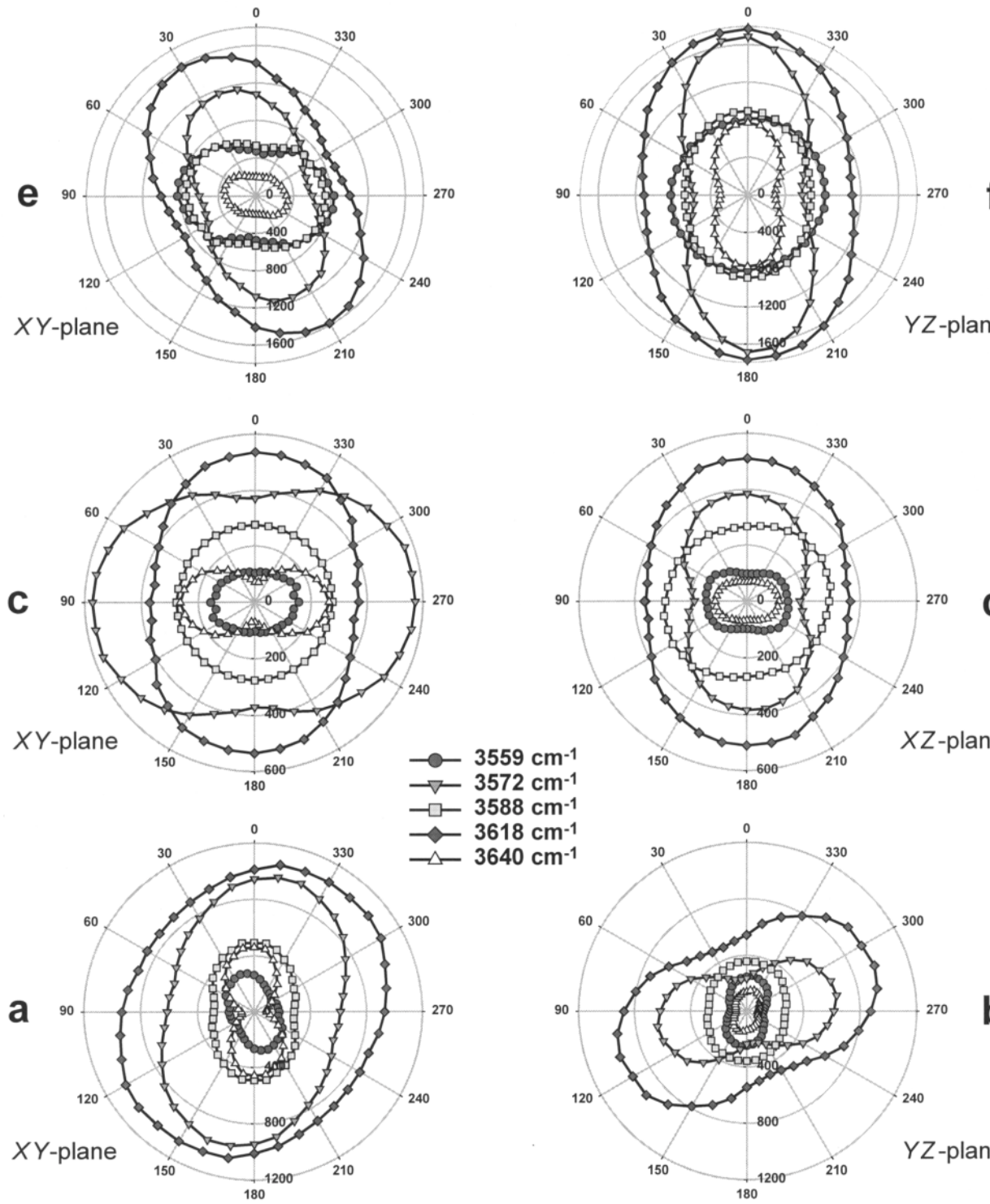

FIGURE 4. OH stretching vibrational absorption of five representative bands from polarized spectra of oriented uvarovite samples. **(a)** Sar-w2, *XY* plane, **(b)** *YZ* plane; **(c)** Sar-899, *XY* plane, **(d)** *XZ* plane; **(e)** Sar-kl2, *XY* plane, **(f)** *YZ* plane.

The calculated water contents of the uvarovites are included in Table 4. Referring to the respective compositions determined by EMP analysis, the water concentration ranges from 0.07 wt% H_2O in Ska-1 to 0.34 wt% H_2O in Sar-kl2. This is equivalent to 0.03 to 0.15 mol% hydrogarnet component. The samples from the Saranov locality exhibit considerably different water contents, despite their being chemically homogeneous.

Discussion

Optical absorption spectroscopy

Electronic *d-d* transitions within $3d^n$ ions are generally dipole transitions and therefore forbidden according to the Laporte selection rule (Ballhausen 1962; Lever 1984). By admixing states with odd parity (e.g., *p*-orbital character) to the *d*-states this selection rule can be relaxed. In acentric complexes, however, parity has no absolute significance due to static removal of the inversion center. In the case of centrosymmetric complexes, the inversion center can only be removed dynamically by vibronic coupling with odd vibrations. Consequently, absorption intensities in centrosymmetric transition metal complexes are weaker than respective transitions in acentric transition metal complexes (Lever 1984). Wildner and Andrut (1998) report the different magnitude of the linear absorption coefficients α for the first spin-allowed transition of $Cr^{3+}O_6$ octahedra in two polymorphs of $Cr(SeO_2OH)(Se_2O_5)$ due to the extent of violation of the Laporte selection rule. In case of a static absence of an inversion center, α was on the order of 500 cm^{-1}, whereas for the centrosymmetric complex α did not exceed 120 cm^{-1} (at room temperature). A comparison with the α values of the uvarovites, which are about 70 cm^{-1} at comparable Cr^{3+} concentration, strongly indicates that the Cr^{3+} cations in uvarovite occupy centrosymmetric sites, regardless of the exact symmetry reduction.

In cubic garnets, Cr^{3+} occupies the octahedrally coordinated site with point symmetry $\bar{3}$. Since the investigated uvarovite crystals are optically biaxial with orthorhombic or lower and most probably centric symmetry, the unique cubic Cr^{3+} position will split into several sites with point symmetry $\bar{1}$ (Wildner and Andrut 2001). Consequently, due to the removal of degeneracy in a low symmetry crystal field, further splitting of energy states and polarization behavior according to the symmetry selection rules is expected (Wilson et al. 1980). Nevertheless, the anisotropic uvarovite crystals still exhibit an isotropic spectral behavior in the visible range. This is attributed to weak distortion of the CrO_6 octahedra in the cubic uvarovite structure (Novak and Gibbs 1971), which is well preserved in our low-symmetry uvarovites (Part II). Accordingly, no splitting of the energy levels (and, of course, no pleochroism in the case of cubic symmetry) was observed so far for uvarovites (Amthauer 1976; Burns 1993; Taran et al. 1994). Amthauer (1976) reports only a slight asymmetry of the spin-allowed bands, similar to the asymmetry of the spin-allowed bands observed in the anisotropic uvarovites under investigation. Within the limits of error, the latter also do not exhibit an increase in FWHM. Furthermore, since in the garnet structure the pseudo-threefold octahedral axes are kinked against each other according to cubic symmetry, the absorption spectrum will consist of contributions from different oriented octahedra for each polarization direction. Hence, apart from the weak distortion of the Cr^{3+} octahedra, the admixture of components of differently oriented octahedra results in an isotropic behavior in the UV-VIS spectral region.

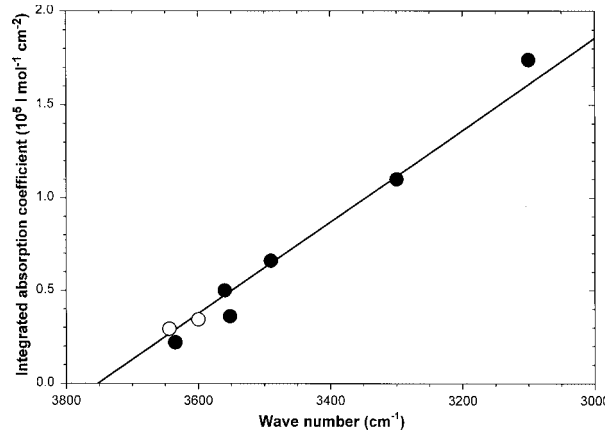

Figure 5. Correlation of the integrated molar absorption coefficient ε of OH stretching bands vs. wave number after Libowitzky and Rossman (1997). Open symbols represent data from Hösch (1999) obtained on Ca-rich garnet samples TSAV and HESS1.

Crystal field strength for Cr^{3+}

As stated above (Eq. 3), according to crystal field theory the field strength parameter 10 *Dq* is correlated with the cation–ligand distance *R* by $1/R^5$. Hence, for a quantitative interpretation the knowledge of mean Cr-O bond lengths is essential. This is problematic since, firstly, no UV-VIS absorption spectra of uvarovites whose crystal structures have also been investigated are available up to now; secondly, due to the nature of the diffraction experiment, the interatomic distances in solid solutions are averaged over all polyhedra of a specific crystallographic site, and hence, do not represent the actual bond lengths in a single polyhedron. In contrast, UV-VIS spectroscopy is sensitive to the individual transition metal and its specific coordination, thus leading to possible discrepancies when comparing the results from diffraction experiments with those of spectroscopic investigations.

In the rare literature on optical spectra of Cr-bearing garnets, the lattice parameter *a* is the only structural information available. This parameter reflects both the expansion/compression of the coordination polyhedra and polyhedral tilting due to cation substitution (Hazen and Finger 1982). Respective available data are compiled for comparison in Figure 6. This figure is a redrawn and supplemented version of Figure 13 in Amthauer (1976). In addition, the synthetic end-member of uvarovite (Bass 1986) was re-investigated. Previous examinations (Abu-Eid 1976; Langer and Abu-Eid 1977) showed a large discrepancy in values for the respective spin-allowed *d-d* transitions. The value of 16667 cm^{-1} given by Abu-Eid (1976), obtained on a powdered sample of synthetic end-member uvarovite, is far too high in view of the value of 16610 cm^{-1} determined for a $gr_{79}uv_{21}$ solid solution (Taran et al. 1994). The former high value not only contradicts the behavior as predicted

by theory, but also the behavior already observed for Cr^{3+} in other oxygen-based phases including synthetic yttrium garnet (Neuhaus 1960; Reinen 1971 and references therein). On the other hand, due to poor data quality, Langer and Abu-Eid (1977) could only report an approximate band position for end-member uvarovite at 15700 cm^{-1} which seems to be a comparatively low value. For the re-investigated synthetic uvarovite from Bass (1986), we determined the barycenters of the first and second spin-allowed bands at 16050 and 22430 cm^{-1}, respectively.

For the uvarovite-grossular binary, Figure 6 exhibits a linear variation of the energy of the first spin-allowed band as a function of the lattice parameter. With increasing Cr/Al ratio, the octahedrally coordinated site is expanded, shifting the band to lower energy (Neuhaus 1960; Amthauer 1976). The anisotropic garnets Sar-899 and Ska-1 with low water content match this relationship. A slight deviation to higher crystal field stabilization energies is observed for samples with higher water concentrations (Sar-desy, Sar-kl2, Sar-w2, and Ves-2). Since no analyses of a possible hydrous component of the other Cr^{3+}-bearing garnets are reported in the literature, it remains questionable if this slight deviation can be really attributed to the water content of these four samples. Pyrope-rich garnets also show a linear dependence of the first spin-allowed band with the lattice constant, but with a different slope compared to the uvarovite-grossular binary. The Cr-bearing pyrope samples from Stockdale represent a nearly binary pyrope- Cr-pyrope join (Rost et al. 1975) and therefore display a perfect correlation. Scattering of the other data is due to the influence of further cations. The observations made above are in accordance with data by Huckenholz and Knittel (1975), who reported an ideal behavior of the lattice parameter *a* along the uvarovite-grossular binary. Ungaretti et al. (1995) also observed an ideal behavior of the structural parameters for binary solid solutions in which the octahedral cation is exchanged. In contrast, non-ideal behavior was observed for most structural parameters in those binaries where Ca was exchanged with Mg, Fe^{2+}, or Mn^{2+} at the dodecahedral site. Therefore, the uvarovite-grossular binary and the pyralspites exhibit different slopes and/or offsets. Additionally, a gap was observed for garnets in the range of the lattice parameter between 11.67 and 11.77 Å, suggesting

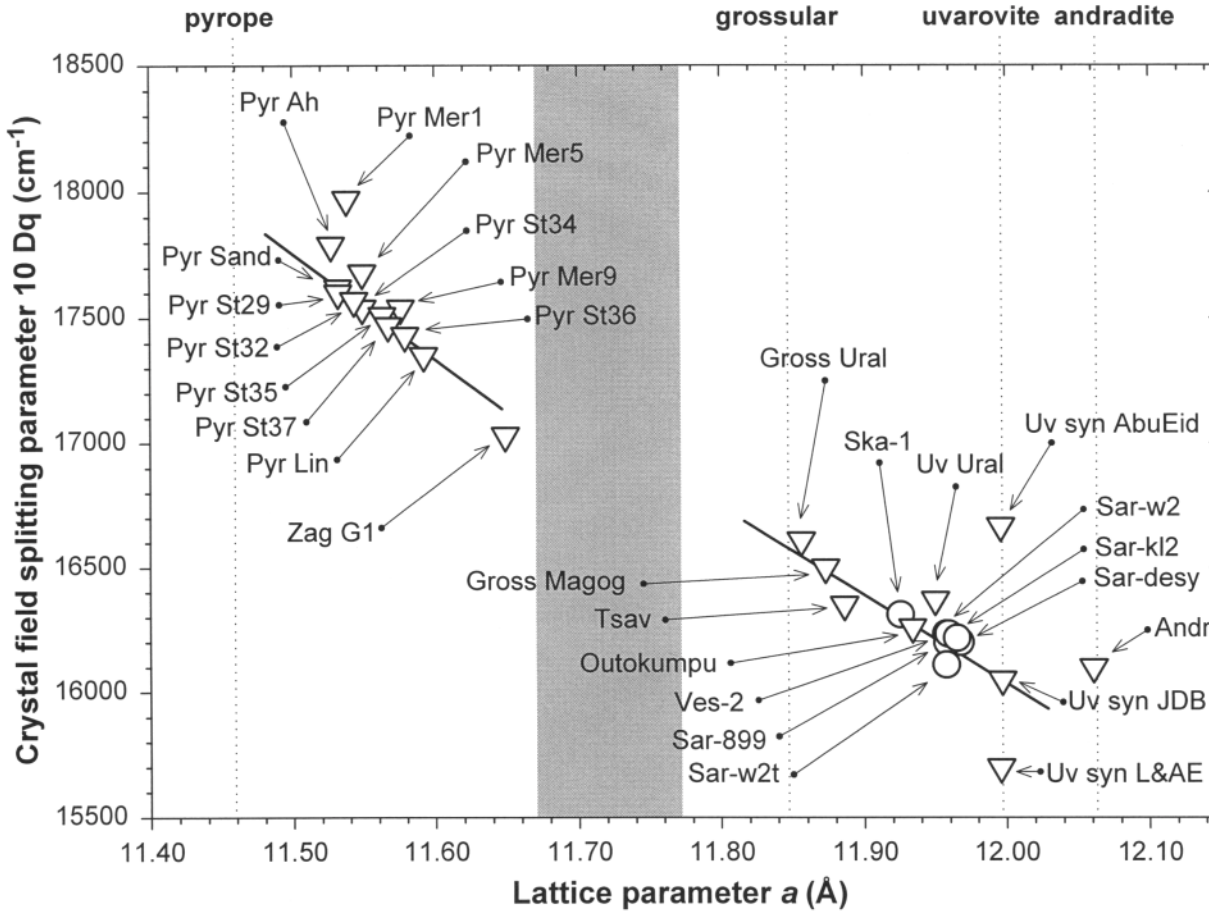

FIGURE 6. Crystal field splitting parameter 10 *Dq* for $^{[6]}Cr^{3+}$ as a function of the lattice parameter of garnet. Circles represent samples of this study, inverted triangles literature data: all Pyr samples, Andr (Val Malenco), Gross Magog, Outokumpu: Amthauer (1976); Tsav: Amthauer (1975); Zag G1: Langer and Andrut (1996); Gross Ural, Uv Ural: Taran et al. (1994); Uv syn AbuEid: Abu-Eid (1976); Uv syn L&AE: Langer and Abu-Eid (1977); Uv syn JDB: synthetic sample from Bass (1986). The lines serve only as a guide for the eyes. For reference, the lattice parameters of the end-members pyrope, grossular, uvarovite and andradite are indicated by vertical lines. The proposed miscibility gap (Ungaretti et al. 1995) between 11.67 and 11.77 Å is indicated by a shaded area.

that this gap will also exist in the correlation depicted in Figure 6.

Hydroxyl stretching vibrations

Reliable IR-spectroscopic data on uvarovite-grossular solid solutions in the region of the OH stretching vibration are practically nonexistent (only a single band position obtained for powder data is given by Heflik and Zabinski 1969). Hence, a thorough interpretation and discussion of possible factors influencing the OH vibrational spectrum of our uvarovites will be facilitated by reference to the much more extensive literature for the grossular-hydrogrossular system. A critical review of the available data reveals that the overall water concentration and the effective local crystal field of the hydroxyl groups, which is controlled by the chemical composition, strongly influences the OH vibrational spectrum. The evaluation of the literature data is difficult because many of the spectra were recorded from powdered samples dispersed in KBr. It has been shown (Rossman and Aines 1991) that bands caused by adsorbed water superimpose the structural OH stretching vibrational signals, leading sometimes to misinterpretations, especially in case of hydrogrossular.

The IR spectrum of synthetic end-member hydrogrossular has been reported by a number of authors (Cohen-Addad et al. 1967; Harmon et al. 1982; Rossman and Aines 1991) to consist at room temperature of a single band located at ~3660 cm^{-1} with a FWHM of ~25 cm^{-1}. Harmon et al. (1982) predict three infrared active T_2 vibrations for tetrahedral molecules of the type X_4H_4 with T_d symmetry, namely one X-H stretching mode, one X-H bending mode and one X···X cage deformation. With decreasing symmetry, the degeneracy of the T_2 state is at least partially lifted. For instance, under S_4, the point symmetry of the O_4H_4 group in the cubic hydrogarnet structure, the T_2 state splits into $B + E$. Both are IR-active, therefore two OH stretching vibrational bands are expected. Based on powder spectra, Cohen-Addad et al. (1967) reported a band splitting only when cooling the sample down to 4 K with split band positions at 3680 and 3590 cm^{-1}. Even at 10 K only one absorption band is observed (Harmon et al. 1982). Contrarily, in the synthetic grossular-hydrogrossular solid solution series, Kobayashi and Shoji (1983) found two OH vibrational bands at ambient conditions at 3660 and 3600 cm^{-1} with intensities systematically varying as a function of composition. Spectra reported for natural intermediate grossular-hydrogrossular solid solutions by Passaglia and Rinaldi (1984) and Rossman and Aines (1991) are consistent with the synthetic spectra. These bands are inevitably assigned to OH-stretching vibrations with different local crystal fields.

Rossman and Aines (1991) attributed the band at 3660 cm^{-1} to O_4H_4 groups that are surrounded by other O_4H_4 groups and the second band at 3600 cm^{-1} to O_4H_4 next to SiO_4 groups. Hence, these two IR signals would correspond to the occurrence of two different types of neighboring domains, i.e., grossular and hydrogrossular. But this interpretation is questionable since the two end-members have very different lattice parameters ($a \approx 11.85$ and 12.57 Å, respectively), which would cause significant structural strain at the proposed domain boundaries.

A closer inspection of the spectra reveals a rather broad and asymmetric shape of the proposed two bands and the presence of shoulders, e.g., in sample 1358 of Rossman and Aines (1991), a single crystal of a "plazolite"-hydrogrossular from Crestmore. Therefore, the spectrum of this sample (original data available from http://minerals.gps.caltech.edu/) was re-examined with special regard to band asymmetry and shoulders, taking into account all possible configurations of O_4H_4 groups (abbreviated as Hy) and SiO_4 tetrahedra (Si) at the four tetrahedral sites of the second polyhedral coordination sphere of an O_4H_4 group (the first polyhedral coordination sphere consists of octahedra and dodecahedra). The following five main configurations can be distinguished: HyHyHyHy, SiHyHyHy, SiSiHyHy, SiSiSiHy, and SiSiSiSi, giving rise to one distinct band each (at ambient temperature and disregarding local symmetry reduction). In the cubic garnet space group $Ia\bar{3}d$ the conformational permutation for each configuration is degenerate except for SiSiHyHy, where two conformations can be distinguished. Using peak-deconvolution methods, five bands—corresponding to the five main configurations—were fitted to the spectrum, thus giving band positions, FWHM, and respective areas (given in percentages). As suggested by Rossman and Aines (1991), the band around 3660 cm^{-1} is obviously caused by O_4H_4 with configuration HyHyHyHy, but accounts for only 24% of the total area. Band positions and respective areas for the other configurations in order of increasing Si "coordination" are 3633 (10%), 3600 (35%), 3577 (25%) and 3542 cm^{-1} (6%). All bands have a FWHM in the order of 35 cm^{-1}. For this "plazolite" hydrogarnet sample, an Si mole fraction of $X_{Si} = 0.51$ was previously determined by Basso et al. (1983). Under the assumption of a random distribution (and neglecting the wavelength-dependency of the linear absorption coefficient in this comparatively narrow spectral range; influence at most ± 1%) the probabilities p_i of the five configurations can be calculated yielding (respective band position in parentheses):

$p_{HyHyHyHy} = (1–X)^4 \quad \equiv 6\%$ (3660 cm^{-1})
$p_{SiHyHyHy} = 4(1–X)^3\, X \equiv 24\%$ (3633 cm^{-1})
$p_{SiSiHyHy} = 6(1–X)^2\, X^2 \equiv 37\%$ (3600 cm^{-1})
$p_{SiSiSiHy} = 4(1–X)\, X^3 \quad \equiv 26\%$ (3577 cm^{-1})
$p_{SiSiSiSi} = X^4 \quad \equiv 7\%$ (3542 cm^{-1})

The results for the prevailing Si environments agree well with the experimental data, whereas the population of the pure hydrogarnet component (i.e., HyHyHyHy) is underestimated, while the SiHyHyHy configuration is overestimated. However, for the interpretation of our uvarovite spectra it is important to re-emphasize from the derivation above and the spectra of Rossman and Aines (1991) that in binary grossular-hydrogrossular solid solutions different configurations on the four nearest tetrahedral sites give rise to OH vibrational bands with their centers scattering by only some 120 cm^{-1} and a barycenter located at around 3600 cm^{-1}.

By analogy with the uvarovite spectra, the spectra of natural, low-water, mostly Fe-bearing grossulars measured by Rossmann and Aines (1991) are much more complicated, consisting of many overlapping bands in the spectral range between 3700 and 3475 cm^{-1}. Obviously, different local cation configurations on structural sites directly adjacent to the O_4H_4 group, i.e., octahedral and dodecahedral, give rise to a number of additional bands and may also cause respective energy shifts.

Furthermore, besides the common hydrogarnet substitution, other substitution mechanisms may be active, a number of which have been proposed, e.g., by Geiger et al. (1991), Langer et al. (1993), Khomenko et al. (1994), or Geiger et al. (2000). However, a correlation of the spectral complexity with composition or formation conditions has not been definitively established.

The uvarovite-grossular solid solutions investigated in the present study all exhibit low water contents. Their IR absorptions due to structurally incorporated OH groups cover a similar spectral range to those of natural grossular samples. Therefore it is concluded that the OH vibrational band splittings are primarily caused by different Cr/Al-cation local configurations at the octahedral positions adjacent to an O_4H_4 group—thus leading to distinct electrostatic as well as geometric distortions of the local field—and secondarily by different SiO_4 and O_4H_4 configurations at the four tetrahedral sites of the second polyhedral coordination sphere. In the garnet structure each O_4H_4-tetrahedron shares its corner O atoms with four octahedra and two O–O edges with dodecahedra. Given a full and uniform occupation of the dodecahedral sites in the investigated uvarovites by Ca (Wildner and Andrut 2001), five different local crystal fields with respect to the octahedral Cr/Al distribution are possible for each O_4H_4 tetrahedron, i.e., the octahedral configurations CrCrCrCr, CrCrCrAl, CrCrAlAl, CrAlAlAl, and AlAlAlAl. Depending on the actual local symmetry, each of these configurations may exhibit different symmetrical and hence energy degeneracies. In triclinic symmetry, for example, all degeneracies are abolished, raising the number of different local crystal fields for each tetrahedron to 16, and thus the number of possible local cation configurations around a central tetrahedron is increased to $6 \times 16 = 96$. In this context, a further band splitting due to distortion of the O_4H_4 tetrahedron in strongly distorted local environments may also be considered: for a completely asymmetric O_4H_4 group, four OH stretching vibrations are expected, theoretically resulting in a total of 384 bands.

In each spectrum of the investigated uvarovite crystals, 14 bands with a FWHM in the order of 15 cm^{-1} were observed in the spectral range 3680 to 3470 cm^{-1}, irrespective of their different orthorhombic, monoclinic or triclinic polarization behavior. That no correlation with symmetry is observed indicates that both effects, i.e., lifting of the degeneracies of the Cr/Al cation configurations as well as splitting according to the six crystallographically different tetrahedra in triclinic symmetry, are too weak to cause a recognizable splitting of the absorption bands, at least at ambient temperatures. Since measurements at 77 K also revealed no further resolution of bands, a band splitting due to low symmetry is expected, by analogy with hydrogrossular, to occur only below 10 K.

A detailed assignment of the 14 OH vibrational bands in our uvarovites is not feasible since important benchmark data are still lacking, e.g., respective band positions and spectral features in synthetic end-member uvarovite and in synthetic "hydrouvarovite." Furthermore, the influence of trace elements, especially associated with defects, cannot be distinguished from "normal" hydrogarnet substitution. EMP analyses revealed that besides Cr, other transition metals are present in traces, i.e., primarily Ti and in sample Ska-1 also Fe. The incorporation of these elements probably leads to defects or vacancies in the garnet structure. Respective coupled substitution mechanisms including hydroxyl incorporation have been proposed (Khomenko et al. 1994), e.g., $^{[6]}Al^{3+} + {}^{[4]}Si^{4+} + 4O^{2-} = {}^{[6]}Ti^{4+} + {}^{[4]}\square + [(OH)_3O]^{5-}$. A study by Geiger et al. (2000) on synthetic pyropes also clearly shows that the incorporation of highly charged elements, which modify the garnet stoichiometry, probably by creating vacancies and/or defects, allows additional OH substitutional mechanisms. In addition, a cation substitution on the dodecahedral position has also to be taken into account, further increasing the possible number of OH bands by creating different local crystal fields in analogy to the substitution on the octahedral positions. On the other hand, the amount of divalent substitutional cations in the uvarovites under investigation is negligible compared to the Cr/Al substitution.

However, some clues to the band assignment may be drawn from the remnant spectrum of the annealed Sar-w2 crystal with four bands located at 3602, 3574, 3556, and 3517 cm^{-1}, yielding steadily increasing absorption intensity. In agreement with a Cr:Al ratio of 1.36:0.60 and a water content of <0.01 wt%, these bands may be assigned to O_4H_4 groups with local octahedral CrAlAlAl, CrCrAlAl, CrCrCrAl, and CrCrCrCr configurations, respectively, and with SiSiSiSi configuration in the second polyhedral coordination sphere in each case. According to the Cr dominance of this sample, O_4H_4 groups with local AlAlAlAl configuration are probably not detectable in the IR spectra.

ACKNOWLEDGMENTS

The authors thank A. Beran and E. Libowitzky (Vienna) for many helpful discussions and valuable comments. F. Brandstätter, Museum of Natural History (Vienna), kindly helped during the electron microprobe analyses, and A. Wagner (Vienna) carefully prepared the crystals. Thanks are further due to R. Wirth (GFZ Potsdam) for the TEM investigations and to J.D. Bass (Urbana) for providing the synthetic uvarovite sample Uv syn JDB. Reviews by B. Chakoumakos and an anonymous reviewer helped to improve the manuscript. M.A. gratefully acknowledges a grant by the Akademie der Naturforscher "Leopoldina," Halle, Germany, and financial support by the Bundesministerium für Bildung und Forschung, Germany.

REFERENCES CITED

Abu-Eid, R.M. (1976) Absorption spectra of transition metal-bearing minerals at high pressures. In R.G.J. Strens, Ed., The physics and chemistry of minerals and rocks. Wiley, New York, 641–675.

Aines, R.D. and Rossman, G.R. (1984) The hydrous component in garnets: pyralspites. American Mineralogist, 69, 1116–1126.

———(1985) The water component of mantle garnets. Geology, 12, 720–723.

Akizuki, M. (1984) Origin of optical variations in grossular-andradite garnet. American Mineralogist, 66, 403–409.

Akizuki, M., Takéuchi, Y., Terada, T., and Kudoh, Y. (1998) Sectoral texture of a cubo-dodecahedral garnet in grandite. Neues Jahrbuch für Mineralogie, Monatshefte, 12, 565–576.

Allen, F.A. and Buseck, P.R. (1988) XRD, FTIR, and TEM studies of optically anisotropic grossular garnets. American Mineralogist, 73, 568–584.

Amthauer, G. (1975) Zur Kristallchemie und Farbe grüner und brauner Grossulare aus Tanzania. Zeitschrift der deutschen Gemmologischen Gesellschaft, 24, 61–72.

———(1976) Kristallchemie und Farbe chromhaltiger Granate. Neues Jahrbuch für Mineralogie, Abhandlungen, 126, 158–186.

Ballhausen, C.J. (1962) Introduction to ligand field theory, 307 p. McGraw-Hill, New York.

Bass, J.D. (1986) Elasticity of uvarovite and andradite garnets. Journal of Geophysical Research, 91, B7, 7505–7516.

Basso, R., Della Giusta, A., and Zefiro, L. (1983) Crystal structure refinement of plazolite: a highly hydrated natural hydrogrossular. Neues Jahrbuch für Mineralogie, Monatshefte, 6, 251–258.

Basso, R., Cimmino, F., and Messiga, B. (1984) Crystal chemistry of hydrogarnets from three different microstructural sites of a basaltic metarodingite from the Voltri Massif (Western Liguria, Italy). Neues Jahrbuch für Mineralogie, 148, Abhandlungen, 246–258.

Bell, D.R., Ihinger, P.D., and Rossman, G.R. (1995) Quantitative analysis of trace

OH in garnet and pyroxenes. American Mineralogist, 80, 465–474.
Beran, A., Langer, K., and Andrut, M. (1993) Single crystal infrared spectra in the range of OH fundamentals of paragenetic garnet, omphacite and kyanite in an eclogitic mantle xenolith. Contributions to Mineralogy and Petrology, 48, 257–268.
Blanc, Y. and Maisonneuve, J. (1973) Sur la biréfringence de la grénats calciques. Bulletin de la Societé Francaise de Minéralogie et de Cristallographie, 96, 320–321.
Brown, D. and Mason, R.A. (1994) An occurrence of sectored birefringence in almandine from the Gangon terrane, Labrador. The Canadian Mineralogist, 32, 105–110.
Burns, R.G. (1993) Mineralogical applications of crystal field theory, ed. 2, 574p. Cambridge University Press, Cambridge.
Chase, A.B. and Lefever, R.A. (1960) Birefringence of synthetic garnets. American Mineralogist, 45, 1126–1129.
Cohen-Addad, C., Ducrois, P., Durif, A., Bertaut, E.F., and Delapalme, A. (1964) Détermination de la position des atomes d'hydrogéne dans l'hydrogrenat $Al_2O_3{\cdot}3CaO{\cdot}6H_2O$ par résonance magnétique nucléare et diffraction neutronique. Journal de Physique, 25, 478–483.
Cohen-Addad, C., Ducrois, P., and Bertaut, E.F. (1967) Étude de la substitution du groupement SiO_4 par $(OH)_4$ dans les composes $Al_2Ca_3(OH)_{12}$ et $AlCa_3(SiO_4)_{2.16}(OH)_{3.36}$ de type grenat. Acta Crystallographica, 23, 220–230.
Foord, E.E. and Mills, B.A. (1978) Biaxiality in 'isometric' and 'dimetric' crystals. American Mineralogist, 63, 316–325.
Foreman, D.W. (1968) Neutron and X-ray diffraction study of $Ca_3Al_2(O_4D_4)_3$. Journal of Chemical Physics, 48, 3037–3041.
Geiger, C.A., Winkler, B., and Langer, K. (1989) Infrared spectra of synthetic almandine-grossular and almandine-pyrope garnet solid solutions: evidence for equivalent site behaviour. Mineralogical Magazine, 53, 231–237.
Geiger, C.A., Langer, K., Bell, D.R., Rossman, G.R., and Winkler, B. (1991) The hydroxide component in synthetic pyrope. American Mineralogist, 76, 49–59.
Geiger, C.A., Stahl, A., and Rossman, G.R. (2000) Single crystal IR- and UV/VIS-spectroscopic measurements on transition-metal-bearing pyrope: the incorporation of hydroxide in garnet. European Journal of Mineralogy, 12, 259–271.
Griffen, D.T., Hatch, D.M., Phillips, W.R., and Kulaksiz, S. (1992) Crystal chemistry and symmetry of a birefringent tetragonal $pyralspite_{75}$-$grandite_{25}$ garnet. American Mineralogist, 77, 399–406.
Griffiths, P.R. and de Haseth, J.A. (1986) Fourier transform infrared spectroscopy, 671 p. Wiley, New York.
Griggs, D.T. and Blacic, J.D. (1964) The strength of quartz in the ductile regime. Transactions of the American Geophysical Union, 45, 102–103.
Harmon, K.M., Gabriele, J.M., and Nutall, A.S. (1982) Hydrogen bonding, Part 14. Hydrogen bonding in the tetrahedral $O_4H_4^{4-}$ cluster in hydrogrossular. Journal of Molecular Structure, 82, 213–219.
Hazen, R.M. and Finger, L.W. (1982) Comparative crystal chemistry. Temperature, pressure, composition and the variation of crystal structure, 248 p. Wiley, New York.
Heflik, W. and Zabinski, W. (1969) A chromian hydrogrossular from Jordanow, Lower Silesia, Poland. Mineralogical Magazine, 37, 241–243.
Hösch, A. (1999) Schwingungsspektropskopie von OH-führenden Defekten in Granaten, Ph.D. dissertation. Technical University, Berlin.
Hofmeister, A.M., Schaal, R.B., Campbell, K.R., Berry, S.L., and Fagan, T.J. (1998) Prevalence and origin of birefringence in 48 garnets from the pyrope-almandine-grossularite-spessartine quaternary. American Mineralogist, 83, 1293–1301.
Huckenholz, H.G. and Knittel, D. (1975) Uvarovite: stability of uvarovite-grossularite solid solution at low pressure. Contributions to Mineralogy and Petrology, 49, 211–232.
Ingerson, E. and Barksdale, J.D. (1943) Iridescent garnet from the Adelaide mining district, Nevada. American Mineralogist, 28, 303–312.
Khomenko, V.M., Langer, K., Beran, A., Koch-Müller, M., and Fehr, T. (1994) Titanium substitution and OH-bearing defects in hydrothermally grown pyrope crystals. Physics and Chemistry of Minerals, 20, 483–488.
Kingma, K.J. and Downs, J.W. (1989) Crystal-structure analysis of a birefringent andradite. American Mineralogist, 74, 1307–1316.
Kitamura, K. and Komatsu, H. (1978) Optical anisotropy associated with growth striation of yttrium garnet, $Y_3(Al,Fe)_5O_{12}$. Kristallographie and Technik, 13, 811–816.
von Knorring, O. (1951) A new occurrence of uvarovite from northern Karelia in Finland. Mineralogical Magazine, 29, 594–601.
Kobayashi, S. and Shoji, T. (1983) Infrared analysis of the grossular-hydrogrossular series. Mineralogical Journal, 11, 331–343.
Koch-Müller, M., Langer, K., and Beran, A. (1995) Polarized single-crystal FTIR-spectra of natural staurolite. Physics and Chemistry of Minerals, 22, 108–114.
Lager, G.A., Armbruster, Th., and Faber, J. (1987) Neutron and X-ray diffraction study of hydrogarnet $Ca_3Al_2(O_4H_4)_3$. American Mineralogist, 72, 758–767.
Lager, G.A., Armbruster, Th., Rotella, F., and Rossman, G.R. (1989) OH substitution in garnets: X-ray and neutron diffraction, infrared, and geometric-modelling studies. American Mineralogist, 74, 840–851.
Langer, K. and Abu-Eid, R.M. (1977) Measurement of the polarized absorption spectra of synthetic transition metal-bearing silicate microcrystals in the spectral range 44000 – 4000 cm^{-1}. Physics and Chemistry of Minerals, 1, 273–299.
Langer, K. and Andrut, M. (1996) The crystal field concept in geosciences: Does the crystal field stabilisation energy of Cr^{3+} rule its intercrystalline partition behaviour?. In M.D. Dyar, C. McCammon and M.W. Schaefer, Eds., Mineral spectroscopy: a tribute to Roger G. Burns, The Geochemical Society Special Publication no. 5, 29–40.
Langer, K., Robarick, E., Sobolev, N.V., Shatsky, V.S., and Wang, W. (1993) Single-crystal spectra of garnets from diamondiferous high-pressure metamorphic rocks from Kazakhstan: indications for OH^-, H_2O and FeTi charge transfer. European Journal of Mineralogy, 5, 1091–1100.
Lessing, P. and Standish, R.P. (1973) Zoned garnet from Crested Butte, Colorado. American Mineralogist, 58, 840–842.
Lever, A.B.P. (1968) Inorganic electronic spectroscopy, ed. 1, 432 p. Elsevier Publishing Company, Amsterdam.
———(1984) Inorganic electronic spectroscopy, ed. 2, 880 p. Elsevier, Amsterdam.
Libowitzky, E. (1999) Correlation of O-H stretching frequencies and O-H···hydrogen bond lengths in minerals. Monatshefte für Chemie, 130, 1047–1059.
Libowitzky, E. and Rossman, G.R. (1997) An IR absorption calibration for water in minerals. American Mineralogist, 82, 1111–1115.
McAloon, B.P. and Hofmeister, A.M. (1993) Single-crystal absorption and reflection infrared spectroscopy of birefringent grossularite-andradite garnets. American Mineralogist, 78, 957–967.
Martin, R.F. and Donnay, G. (1972) Hydroxyl in the mantle. American Mineralogist, 57, 554–570.
Manning, P.G. (1969) Optical studies of grossular, andradite (var. colophonite) and uvarovite. Canadian Mineralogist, 9, 723–729.
Moore, R.K. and White, W.B. (1972) Electronic spectra of transition metal ions in silicate garnets. Canadian Mineralogist, 11, 791–811.
Neuhaus, A. (1960) Über die Ionenfarben der Kristalle und Minerale am Beispiel der Chromfärbungen. Zeitschrift für Kristallographie, 113, 195–233.
Novak, G.A. and Gibbs, G.V. (1971) The crystal chemistry of the silicate garnets. American Mineralogist, 56, 791–825.
Pavlov, N.V. and Grigor'eva, I.I. (1977) Deposits of chromium. In V. I. Smirnov: Ore deposits of the USSR, Vol. 1, 179–236. Pittman publishing, London.
Passaglia, E. and Rinaldi, R. (1984) Katoite, a new member of the $Ca_3Al_2(SiO_4)_3$–$Ca_3Al_2(OH)_{12}$ series and new nomenclature for the hydrogrossular group of minerals. Bulletin de Minéralogie, 107, 605–618.
Perumareddi, J.R. (1967) Ligand field theory of d3 and d7 electronic configurations in non-cubic fields I: Wave function and energy matrices. Journal of Physical Chemistry, 71, 3144–3154.
Racah, G. (1942) Theory of complex spectra I. Physical Reviews, 61, 186–197.
Reinen, D. (1971) Ligand field spectroscopy and chemical bonding in Cr^{3+}-containing oxidic solids. Structure and Bonding, 6, 114–154.
Rost, F., Beerman, E., and Amthauer, G. (1975) Chemical investigation of pyrope garnets in the Stockdale kimberlite intrusion, Riley County, Kansas. American Mineralogist, 60, 675–680.
Rossman, G.R. and Aines, R.D. (1986) Spectroscopy of a birefringent grossular from Asbestos, Quebec, Canada. American Mineralogist, 71,779–780.
———(1991) The hydrous component in garnets: Grossular-hydrogrossular. American Mineralogist, 76, 1153–1164.
Schläfer, H.L. and Gliemann, G. (1980) Einführung in die Ligandenfeldtheorie, ed. 2, 549 p. Akademische Verlagsgesellschaft, Frankfurt/Main.
Tanabe, Y. and Sugano, S. (1954) On the absorption spectra of complex ions I. Journal of the Physical Society of Japan, 9, 753–766.
Takéuchi, Y., Haga, N., Umizu, S., and Sato, G. (1982) The derivative structure of silicate garnets in grandite. Zeitschrift für Kristallographie, 158, 53–99.
Taran, M.N., Langer, K., Platonov, A.N., and Indutny, V.V. (1994) Optical absorption investigation of Cr^{3+} ion-bearing minerals in the temperature range 77–797 K. Physics and Chemistry of Minerals, 21, 360–372.
Thompson, A.B. (1992) Water in the earth's upper mantle. Nature, 358, 295–302.
Ungaretti, L., Leona, M., Merli, M., and Oberti, R. (1995) Non-ideal solid-solution in garnet: crystal structure evidence and modeling. European. Journal of Mineralogy, 7, 1299–1312.
Wildner, M. (1996) Tetrig—a program for calculating spin-allowed energy levels of d^2, d^3, d^7, and d^8 ions in tetragonal and trigonal crystal fields. Abstracts of the 3rd European Meeting on Spectroscopic Methods in Mineralogy, Kiev.
Wildner, M. and Andrut, M. (1998) Crystal structures and electronic absorption spectra of two modifications of $Cr(SeO_2OH)(Se_2O_5)$. Journal of Solid State Chemistry, 135, 70–77.
Wildner, M. and Andrut, M. (2001) The crystal chemistry of birefringent natural uvarovites. Part II. Single crystal X-ray structures. American Mineralogist, 86, 1231–1251.
Wilson, E.B., Decius, J.C., and Cross, P.C. (1980) Molecular Vibrations, 399 p. (Unabridged and corrected republication from 1955 by McGraw-Hill.) Dover Publications Inc, New York.

MANUSCRIPT RECEIVED NOVEMBER 7, 2000
MANUSCRIPT ACCEPTED JUNE 14, 2001
MANUSCRIPT HANDLED BY BRYAN CHAKOUMAKOS